Inverse quasifission in the reactions ^{156,160}Gd + ^{186}W

E. M. Kozulin,[1] V. I. Zagrebaev,[1,*] G. N. Knyazheva,[1] I. M. Itkis,[1] K. V. Novikov,[1] M. G. Itkis,[1] S. N. Dmitriev,[1] I. M. Harca,[1,2,3] A. E. Bondarchenko,[1] A. V. Karpov,[1] V. V. Saiko,[1] and E. Vardaci[4]

[1]*Flerov Laboratory of Nuclear Reactions, Joint Institute for Nuclear Research, 141980 Dubna, Russia*

[2]*Faculty of Physics, University of Bucharest, Romania*

[3]*Horia Hulubei National Institute for R&D in Physics and Nuclear Engineering (IFIN-HH), Bucharest-Magurele, Romania*

[4]*Istituto Nazionale di Fisica Nucleare and Dipartimento di Scienze Fisiche dell'Università di Napoli, Napoli, Italy*

(Received 25 September 2017; published 28 December 2017; corrected 22 January 2018)

Background: Low-energy multinucleon transfer reactions may be used for production of new neutron-enriched heavy nuclei.

Purpose: Our aim is to investigate the influence of proton ($Z = 82$) and neutron ($N = 82$, 126) shells as well as orientation effects on the formation of reaction products in the inverse quasifission process in the reactions ^{156,160}Gd + ^{186}W.

Methods: Mass, energy, and angular distributions of primary binary fragments formed in the reactions ^{156}Gd + ^{186}W at an energy of 878 MeV, and ^{160}Gd + ^{186}W at 860 and 935 MeV, have been measured using the double-arm time-of-flight spectrometer CORSET at the U400 cyclotron of the Flerov Laboratory of Nuclear Reactions (FLNR) at the Joint Institute for Nuclear Research (JINR), Dubna.

Results: Enhancement in the yield of products with masses 200–215 u has been found for both reactions. The cross sections of the formation of trans-target fragments with masses around 208 u are found to be about 10 μb at the Coulomb barrier energy and reach the level of 0.5 mb at the energy above the barrier for side-to-side collision.

Conclusions: The enhanced yield of products with masses heavier than the target mass confirms the important role of the closed shells at $Z = 82$ and $N = 82$, 126 in the inverse quasifission process in low-energy damped collisions. The orientation effect caused by the strong deformation of colliding nuclei can result in a gain in the yield of heavy target-like fragments.

DOI: 10.1103/PhysRevC.96.064621

I. INTRODUCTION

In superheavy composite systems formed in reactions with heavy nuclei, the quasifission process (QF) is usually dominant and mainly leads to the formation of asymmetric fragments, which is connected to influence of the shell structure of the driving potential (in particular, the deep valley caused by the double shell closure $Z = 82$ and $N = 126$—double magic lead) on nucleon rearrangement between primary fragments [1,2]. For these systems the entrance channel mass asymmetry is larger than the exit channel one (governed by the double magic lead shell) and nucleons are transferred from the heavier to the lighter nucleus. For more symmetric collisions, nucleons have to be transferred from the lighter to the heavier nucleus to form lead-like nuclei in QF process. This type of QF is the so-called inverse quasifission [3,4]. In inverse QF the final mass asymmetry is larger than the initial one, whereas normal QF tends to reduce this asymmetry. The lead valley evidently reveals itself in both cases.

Several years ago, on the basis of a multidimensional model, it was proposed to use multinucleon transfer reactions, in particular inverse QF, to produce new neutron-rich heavy and superheavy nuclei at bombarding energies close to the Coulomb barrier [5–7]. At the interaction energy near the Coulomb barrier, the formed primary fragments have the lowest possible excitation energy that give them a chance to survive against fission and still remain neutron-rich after their deexcitation via neutron emission. This theoretical study proposes that proton and neutron (independent) flows strongly depend on the shell structure of the multidimensional potential energy surface and the values of fundamental parameters that guide the nuclear dynamics, such as nuclear viscosity. According to the calculations, in the lead region an increased yield of target-like fragments (TLF) formed in the ^{160}Gd + ^{186}W reaction should be observed [4].

In Fig. 1 the potential energies at the contact point in dependence on the fragment mass, calculated for the ^{156,160}Gd + ^{186}W composite systems using the proximity model with NRV code [8], are shown. The upward arrows indicate the projectile and the target masses. The deep minima in the potential energy surface corresponding to the ^{138}Ba + ^{208}Pb configuration are due to the influence of the neutron ($N = 82$, 126) and proton ($Z = 82$) shell closures. As follows from the theoretical calculations, at energies near the Coulomb barrier shell effects can lead to the considerable enhancement of the yield of reaction products with transfer of up to twenty (and even more) nucleons.

This theoretical prediction has been partly confirmed by an experiment. In the radiochemical study of the products formed in the reaction ^{160}Gd + ^{186}W at center-of-mass energy of $E_{\mathrm{c.m.}} = 461.9$ MeV the enhanced yields of trans-target nuclides in the region of gold isotopes were observed, which is in strong contrast with the usual abrupt decrease of the

[*]Deceased.

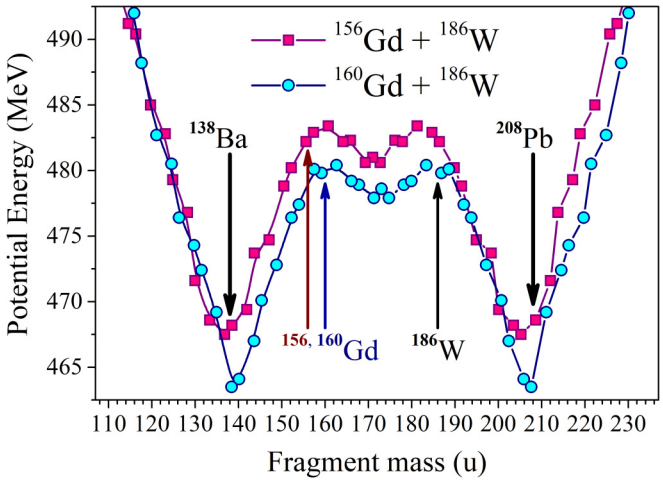

FIG. 1. Potential energy at contact point as a function of the primary fragment mass in the reactions ^{156,160}Gd + ^{186}W.

trans-target product yields [9]. Nevertheless, no fragments with $Z \sim 82$ have been observed in the experiment and it was established that the yield of Pb-like nuclei is at least two orders of magnitude lower than it was predicted in Ref. [4].

Moreover, a net mass transfer from projectile to target of about 20–25 nucleons has been observed in the reaction ^{88}Sr + ^{176}Yb at an energy close to the Coulomb barrier [10]. It was found that the yield of heavy fragments with masses heavier than 190 u is half an order of magnitude larger than may be expected from the extrapolation of an exponential-like behavior of the fragment yields from the region of no-shell closures (mass ∼176 u) to the region of shell closures. The enhanced yield of fragments with masses around 190–200 u is caused by the proton shells at $Z = 28$ and $Z = 82$.

In this paper, the influence of the closed shells on the formation of inverse QF fragments is studied. The reactions ^{156,160}Gd + ^{186}W with two isotopes of Gd were chosen to investigate the influence of neutron excess in the composite system on the formation probabilities and the excitation energies of fragments. The primary mass, energy, and angular distributions of binary fragments have been measured using the double velocities method. The method allows us to measure the primary fragments mass distributions directly and reliably separate the binary reaction channel from products of sequential fission and incomplete fusion reactions and from induced fission of target and target-like nuclei, and does not depend on the lifetime of reaction fragments. Despite this technique not allowing measurement of fragment charge directly, the most probable charge can be derived from the measured mass using the simple assumption of charge/mass equilibration.

II. EXPERIMENT

The experiment was carried out at the Flerov Laboratory of Nuclear Reactions at the U400 cyclotron. A beam of 878 MeV ^{156}Gd and 860, 935 MeV ^{160}Gd ions struck a layer of 150 μg/cm^2 ^{186}W (99.9% enriched) deposited on 50 μg/cm^2 carbon backing. Beam intensity on target was about 20 nA.

Two reaction products were detected in coincidence by the double-arm time-of-flight spectrometer CORSET [11]. Each arm of the spectrometer consists of a compact start detector and a position-sensitive stop detector, both based on microchannel plates. The distance between start and stop detectors was 20 cm. Start detectors were placed at a distance of 3.5 cm from the target. The acceptance of the spectrometer was ±10° in the reaction plane. The angular resolution of the stop detectors is 0.3°. The spectrometer arms were positioned in an optimal way according to the kinematics of the reaction and their angles were changed several times during the experiment. This arrangement allows detecting the coincident binary fragments over an angular range of 25°−65° in the laboratory frame that corresponds to the center-of-mass angle range of 40°−140°. The differential cross sections of primary binary fragments were obtained by normalization to elastic scattering detected by CORSET and by the current integration by means of a Faraday cup.

Primary masses, velocities, energies, and angles in the center-of-mass system of reaction products were calculated from measured velocities and angles using the momentum and energy conservation laws with the assumption that the mass of the composite system is equal to $M_{\text{target}} + M_{\text{projectile}}$. Extraction of the binary reaction channels with full momentum transfer was based on the analysis of the kinematics diagram (see [11,12] for details). The mass and energy resolutions of the present CORSET setup, which define the bin width of the experimental mass and energy yield curves, are taken as the FWHM of the mass and energy spectra constructed for the elastic scattering. In the above conditions, the mass resolution of the spectrometer is ±3 u; the total kinetic energy resolution is ±10 MeV.

III. RESULTS AND DISCUSSION

Mass-TKE (total kinetic energy) distributions of primary binary fragments at energies near the Coulomb barrier are shown in Fig. 2. The energy-dependent characteristics for the reactions under study are presented in Table I.

It is clearly seen from Fig. 2 that, besides the elastic and quasielastic components, a significant number of events have a large dissipation of the initial kinetic energy that indicates the presence of strongly damped collisions for both studied reactions.

The distributions of the total kinetic energy losses (TKEL = $E_{\text{c.m.}}$ − TKE) for all reaction fragments are shown in Fig. 3. Lower TKEL values correspond to quasielastic processes, higher TKEL values correspond to more damped events. If we use a Gaussian curve to reasonably take into account the quasielastic component we observe that most of the damped events are localized at TKEL values above 25 MeV. The cross sections σ_R^{exp} of the damped events were deduced by integrating these energy distributions after removing the quasielastic component (Gaussian curve). The results are presented in Table I. The values of σ_R^{exp} are close to the total reaction cross section σ_R. The large energy damping observed in deep-inelastic reactions suggests an enhanced sticking time of the composite system before reseparation. The estimation of time scale for damped collision gives a

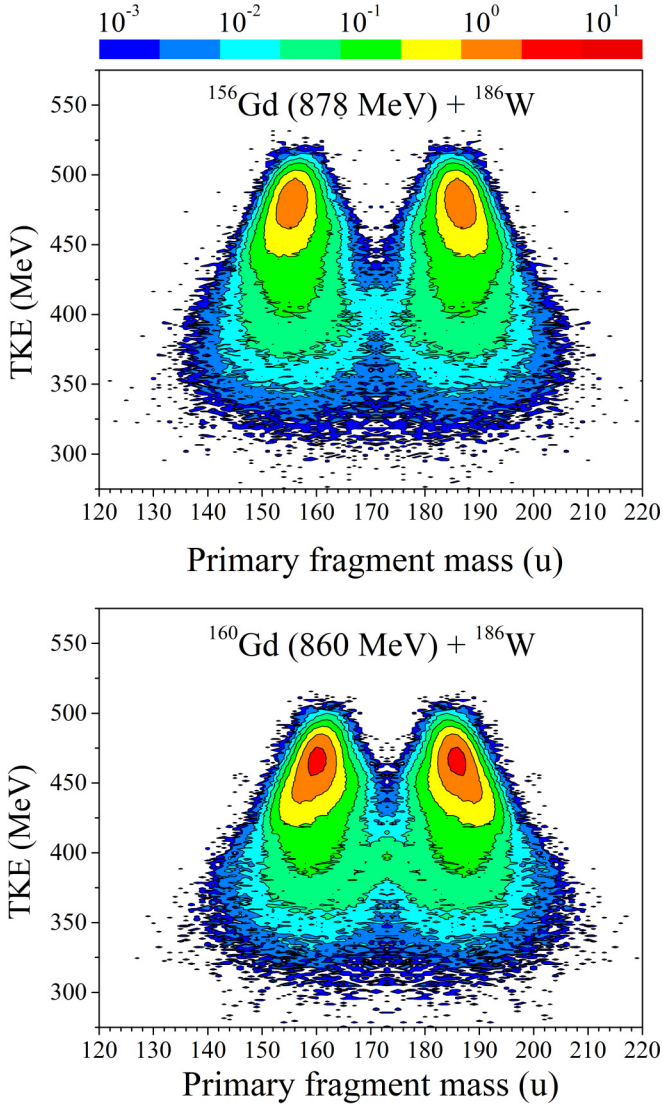

FIG. 2. Mass-energy distributions of the primary binary fragments obtained in the reactions ^{156,160}Gd + ^{186}W at collision energies of 878 and 860 MeV, respectively, and integrated over the angular range of 40°−140° in the center-of-mass system.

time range $10^{-21} - 10^{-20}$ s [7,14–16]. This time is enough to reach large mass transfer among the interacting nuclei. The TKEL distribution for the fragments with mass heavier than 200 u is also shown in Fig. 3. In the case of ^{156}Gd ions the maximum TKEL is about 175 MeV and average TKEL is 103 ± 3 MeV, whereas in the case of ^{160}Gd maximum TKEL is about 140 MeV and its average value is 92 ± 3 MeV.

In Fig. 4 the angular distributions for the trans-target fragments with mass larger than 200 u formed in the reactions ^{156,160}Gd + ^{186}W are shown. The maximum cross section for the formation of these fragments peaks near the grazing angles for TLFs that is a specific feature of deep-inelastic collisions [7,13,17,18]. The width (FWHM) of the angular distribution is ±3.8° for both reactions. The formation cross sections σ^{TLF} of fragments heavier than 200 u, presented in Table I, have been obtained by integrating their angular distributions.

TABLE I. Energy-dependent characteristics for the reactions under study. $\theta^{\mathrm{lab}}_{\mathrm{grazing}}$ is the grazing angle in the laboratory system and L_{grazing} is the grazing angular momentum (calculated using the NRV code [8]), σ_R is the reaction cross section [13], σ_R^{exp} is experimental cross section for damped events, $\theta^{\mathrm{TLF}}_{\mathrm{max}}$ (mass > 200 u) and σ^{TLF} (mass > 200 u) are the laboratory angle for maximum yield and production cross section for TLF fragments with masses heavier than 200 u.

Reaction	^{156}Gd + ^{186}W	^{160}Gd + ^{186}W	^{160}Gd + ^{186}W
E_{lab} (MeV)	878 ± 5	860 ± 5	935 ± 10
$E_{\mathrm{c.m.}}$ (MeV)	477.5	462.3	502.6
E_B (MeV)	474.0	463.4	463.4
$E_{\mathrm{c.m.}}/E_B$	1.007	0.998	1.085
$\theta^{\mathrm{lab}}_{\mathrm{grazing}}$ for Gd (deg)	71.7	75.7	57.0
$\theta^{\mathrm{lab}}_{\mathrm{grazing}}$ for W (deg)	27.3	23.9	38.4
L_{grazing} ($\hbar$)	181	142	244
σ_R (mb)	534	330	908
σ_R^{exp} (mb)	516 ± 50	370 ± 50	950 ± 100
$\theta^{\mathrm{TLF}}_{\mathrm{max}}$ (mass > 200 u) (deg)	28.5 ± 2	26 ± 2	35 ± 2
σ^{TLF} (mass > 200 u) (mb)	2.2 ± 0.4	1.8 ± 0.4	20 ± 5

In Fig. 5 the mass distributions of heavy binary fragments formed in the reactions ^{156,160}Gd + ^{186}W as well as for the ^{136}Xe + ^{208}Pb reaction (see Ref. [18]) at energy close to the Coulomb barrier are presented. In the case of the Xe + Pb reaction, where the influence of closed shells on the formation of trans-target fragments is not expected, the exponential decrease of the cross section with increasing fragment mass is observed (solid line in Fig. 5), whereas for Gd + W one can see a considerable deviation from this exponential dependency in the mass region $A > 200$ u connected with the influence of proton and neutron shells. The mass distributions of heavy primary fragments with TKEL > 50 MeV for the ^{156,160}Gd + ^{186}W reactions are also shown in Fig. 5. Due to such selection of TKEL, most of the quasielastic events have been removed. The mass distributions for both reactions have a two-humped shape with a heavy fragments peak near 186–188 u. The yields of fragments with masses near 208 u ("lead" region) are about 10 μb for both reactions and about two orders of magnitude lower than for fragments in the "gold" region (masses around 200 u). It is exactly the same trend found in the radiochemical experiment [9].

We estimate the available excitation energy of both fragments as $E^*_f = E_{\mathrm{c.m.}} - \mathrm{TKE} + Q_{\mathrm{gg}}$ and assume that this excitation is divided between two primary fragments proportionally to their masses [19]. The distributions of obtained excitation energy for each fragment are shown in Fig. 6. For trans-target fragments heavier than 200 u the excitation is about 60–90 MeV in the case of the ^{156}Gd-induced reaction and 40–70 MeV for ^{160}Gd ions, which leads to the higher survival probability against fission in the second case. Therefore, in the reaction with ^{160}Gd ions, nuclei in the "lead" region evaporate

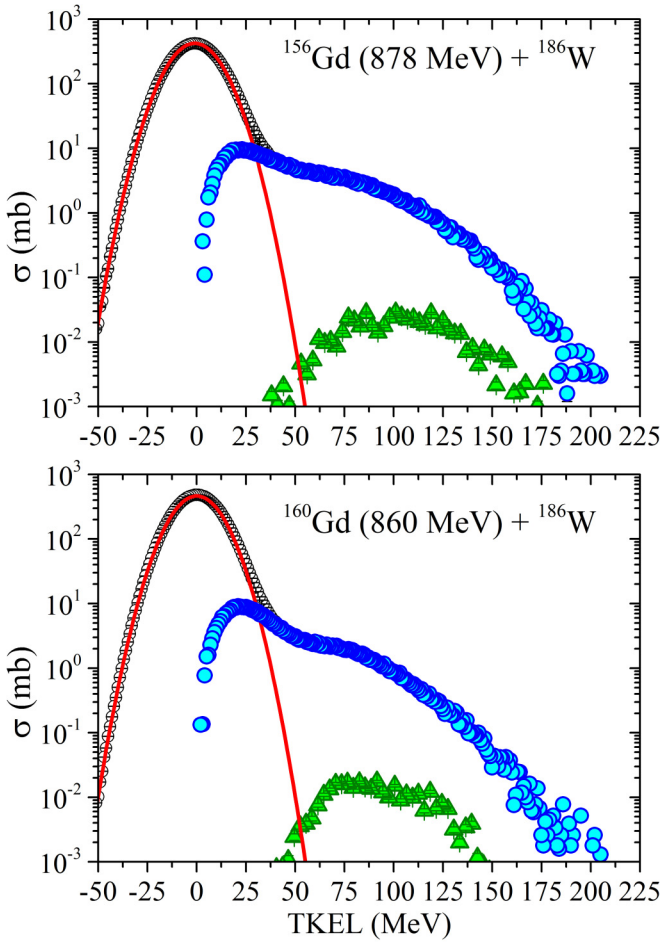

FIG. 3. TKEL distributions of the ^{156,160}Gd + ^{186}W reactions at collision energies of 878 and 860 MeV. The open circles are the TKEL for all events; lines are the elastic and quasielastic (Gaussian-like) contributions; filled circles are TKEL for damped events; triangles are the TKEL for fragments with mass larger than 200 u.

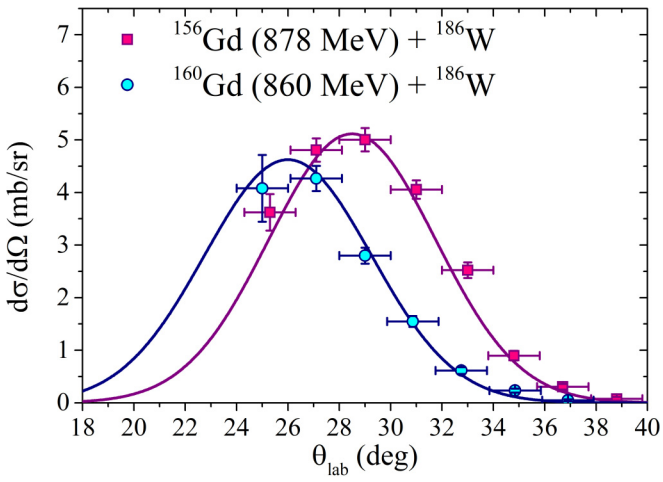

FIG. 4. Laboratory angular distributions of the reaction products with mass larger than 200 u for the reactions ^{156,160}Gd + ^{186}W at E_{lab} = 878 and 860 MeV, respectively.

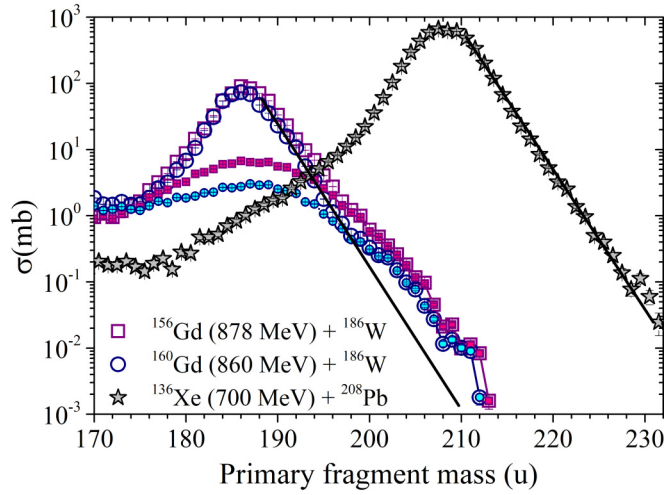

FIG. 5. Mass distributions of all primary binary fragments (open symbols) and for events with energy losses more than 50 MeV (filled symbols) for the reactions ^{156,160}Gd + ^{186}W at E_{lab} = 878 (squares) and 860 MeV (circles). Mass distributions of primary binary fragments formed in the reaction ^{136}Xe + ^{208}Pb at E_{lab} = 700 MeV (stars).

fewer neutrons during their deexcitation than in the case of ^{156}Gd and, consequently, the nuclei formed in the reaction with ^{160}Gd are more neutron-rich.

IV. INFLUENCE OF RELATIVE ORIENTATION OF COLLIDING NUCLEI ON MULTINICLEON TRANSFER CROSS SECTIONS

As was mentioned above, the measurements at the Coulomb barrier energy are preferable to achieve the minimal excitation of primary fragments. Nevertheless, we should note that both Gd and W are strongly deformed nuclei. It is known that in the reactions with well-deformed nuclei their mutual orientation affects considerably the reaction dynamics [20–24].

In Fig. 7 the calculations of potential energy surface are presented for different orientations of interaction nuclei: nose-to-nose, nose-to-side, side-to-nose, and side-to-side. The potential energy surfaces have been calculated within the extended version of the two-center shell model [25] for zero value of unified deformation (i.e., assuming ground-state deformations for separated nuclei and a smooth transition to the ground-state deformation of a compound nucleus for the mononucleus stage). The simplest case is the one corresponding to nose-to-nose orientation, when the system has axial symmetry on each step of its evolution. For arbitrarily oriented nuclei, the calculation of the potential energy is a rather complicated and yet-unsolved problem. The orientation effects can be easily taken into account for separated nuclei, where the potential energy is calculated using the double-folding procedure with Migdal forces [25,26]. After the contact, the potential energy depends on the interaction time. In particular, the axial symmetry should be restored if the interaction time is long enough. The corresponding axially symmetrical shapes are chosen assuming that the nuclear system preserves its compactness during the transition from an axially-asymmetric

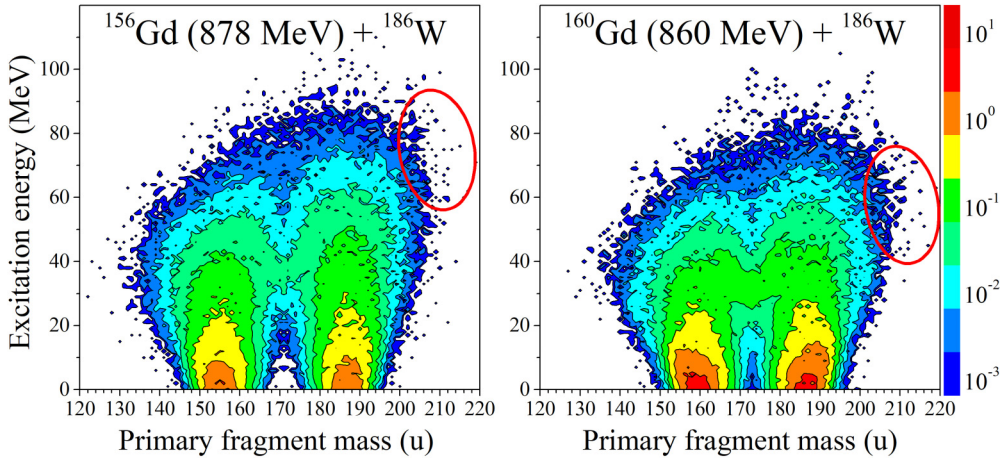

FIG. 6. Excitation energy of primary fragments formed in the reactions ^{156,160}Gd + ^{186}W at collision energies of 878 and 860 MeV, respectively.

configuration (e.g., side-to-side) to an axially-symmetric one. This allows one to have approximately the same interaction potential before and after the symmetry restoration.

One can see from Fig. 7 that in the case of nose-to-nose orientation, due to the position of the contact point on the driving potential, the probability of reaching the valley leading to the formation of the Ba/Pb fragments is extremely low. In the case of nose-to-side collisions this probability increases, although it is still small. For side-to-nose collisions both ways are possible and the composite system can follow either the valley leading to the formation of symmetric fragments or the Ba/Pb valley. For side-to-side configuration the barrier preventing the decay of the system into symmetric fragments appears, and the system evolves along the valley leading to the formation of a Ba/Pb pair.

The interaction energies chosen in the experiment are close to the Coulomb barrier for collisions of spherical nuclei. These energies are higher than the barriers for the nose-to-nose, nose-to-side, and side-to-nose configurations, but much lower than the barrier for the side-to-side configuration. This strongly

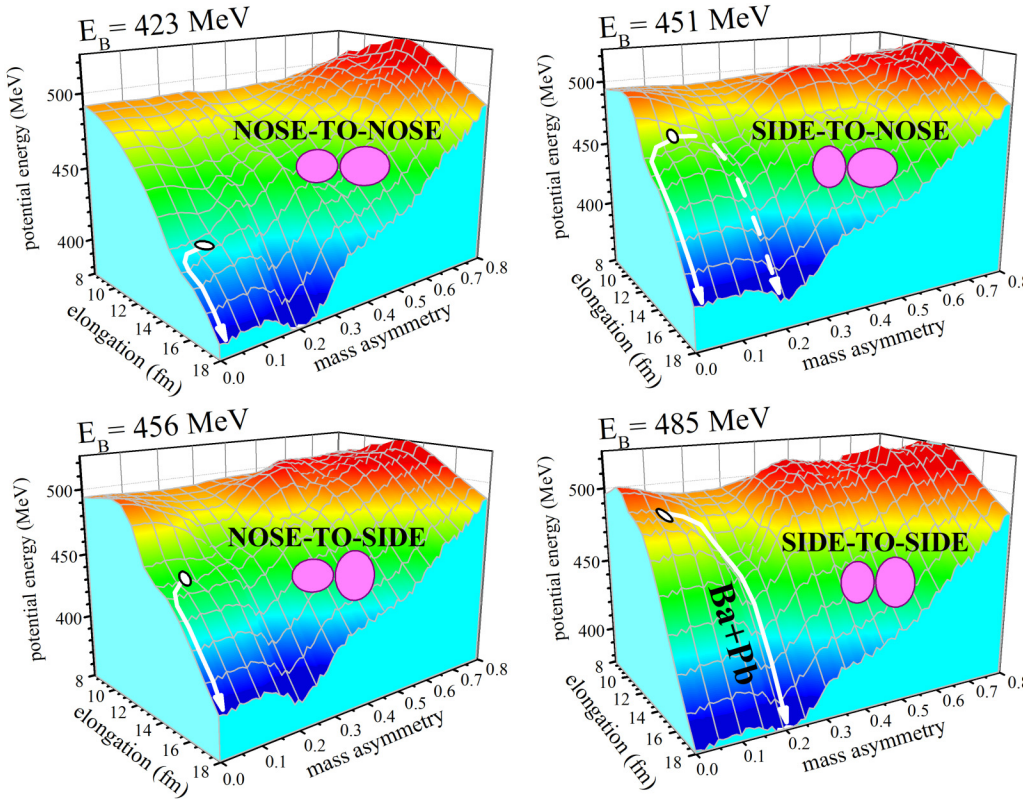

FIG. 7. Potential energy surfaces for the reaction ^{160}Gd + ^{186}W calculated for nose-to-nose, nose-to-side, side-to-nose, and side-to-side orientations of colliding nuclei. The barrier energies for these configurations are indicated at the top of each plot.

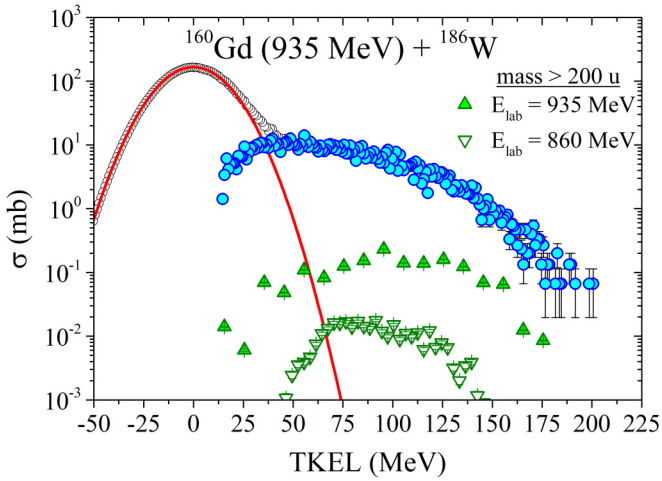

FIG. 8. TKEL distributions of the ^{160}Gd + ^{186}W reaction at a collision energy of 935 MeV. The open circles are the TKEL for all events; lines are the elastic and quasielastic contributions; filled circles are TKEL for damped events; filled and open triangles are the TKEL for fragments with mass larger than 200 u at $E_{lab} = 935$ and 860 MeV, respectively.

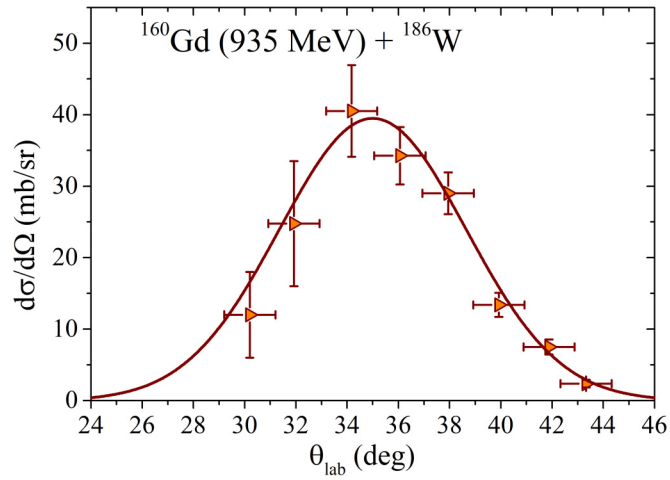

FIG. 9. Laboratory angular distributions of the reaction products with mass larger than 200 u for the reaction ^{160}Gd + ^{186}W at $E_{lab} =$ 935 MeV.

suppresses the nucleon transfer in a wide orientation angle range of both the target and the projectile. From the calculated driving potential for side-to-side collisions one can see that this configuration is the most favorable for the formation of Pb-like fragments, but increasing the collision energy increases the excitation energies of reaction fragments.

To investigate the influence of mutual target-projectile orientation on the formation of trans-target fragments and their excitation energies we measured the mass, energy, and angular distributions of fragments formed in the ^{160}Gd + ^{186}W reaction at a beam energy of 935 MeV, which is about 3.6% higher than the barrier for the side-to-side collisions. At this energy all possible orientations of interacting nuclei give a contribution to reaction fragments formation. The spectrometer arms were positioned at angles of grazing collisions at this beam energy. The reaction products were detected in an angular range of 29°−50° (44°−66° for the complementary fragment) in the laboratory frame. Since the maximum cross section of damped events is located at angles of grazing collisions, this arrangement allows us to detect the majority of all damped events.

The distributions of TKEL for fragments formed in the reaction ^{160}Gd + ^{186}W at $E_{lab} = 935$ MeV are shown in Fig. 8. As expected, the TKEL is higher compared to the distribution at $E_{lab} = 860$ MeV. The distribution for target-like fragments heavier than 200 u extends up to ∼175 MeV at high projectile energy and up to ∼140 MeV for the energy near the Coulomb barrier. Nevertheless, the average TKEL for fragments with mass larger than 200 u is 100 ± 3 MeV. This value is about 10 MeV higher than the one at $E_{lab} = 860$ MeV. This may indicate that the mass transfer in the antisymmetrizing direction proceeds at side-to-side orientations with larger probability because larger values of the contact point potential for this orientation lead to smaller energy losses.

The angular distribution of target-like fragments heavier than 200 u for the reaction ^{160}Gd + ^{186}W at $E_{lab} = 935$ MeV is presented in Fig. 9. As in the case of ^{160}Gd + ^{186}W at $E_{lab} =$ 860 MeV, the maximum production cross section of target-like nuclei peaks near the angle of grazing collisions. The formation cross section of trans-target nuclei heavier than 200 u, obtained by integrating their angular distribution, is one order of magnitude higher than the cross section at $E_{lab} = 860$ MeV while the reaction cross section increases only ∼2.6 times. Thus, along with a relatively small increase of TKEL, an enhancement in the production cross section of these nuclei makes the energy above the barrier for side-to-side collisions more favorable than the energies near the Coulomb barrier for spherical nuclei. Note that, in contrast to ^{160}Gd + ^{186}W, in the reaction with spherical nuclei ^{136}Xe + ^{208}Pb the cross section increases with increasing interaction energy whereas the shape of the mass distribution of fragments virtually does not change [18].

In Fig. 10 the mass distribution for all binary events formed in the reaction ^{160}Gd + ^{186}W at $E_{lab} = 935$ MeV is presented. The mass distributions of fragments with TKEL > 50 MeV obtained in the reaction ^{160}Gd + ^{186}W at two interaction energies, 860 and 935 MeV, are compared. Based on the simple assumption of charge/mass equilibration, the fragments' masses corresponding to the closed shells at $Z = 82$ and $N = 82$, 126 were calculated (see arrows in Fig. 10). The line indicates the tendency of the cross section to decrease exponentially with increasing fragment mass, expected for multinucleon transfer reactions without taking into account shell effects. It is clearly seen that for the fragments heavier than 195 u the experimental cross section is much higher than this exponential tendency due to the influence of the closed shells at $Z = 82$ and $N = 82$, 126. Whereas at $E_{lab} =$ 935 MeV the cross section of fragments with masses heavier than 200 u is about one order of magnitude higher compared to the case of near-Coulomb-barrier measurements, an increase in production cross section of fragments with mass ∼208 u is even stronger, namely, ∼500 μb for $E_{lab} = 935$ MeV and ∼10 μb for $E_{lab} = 860$ MeV.

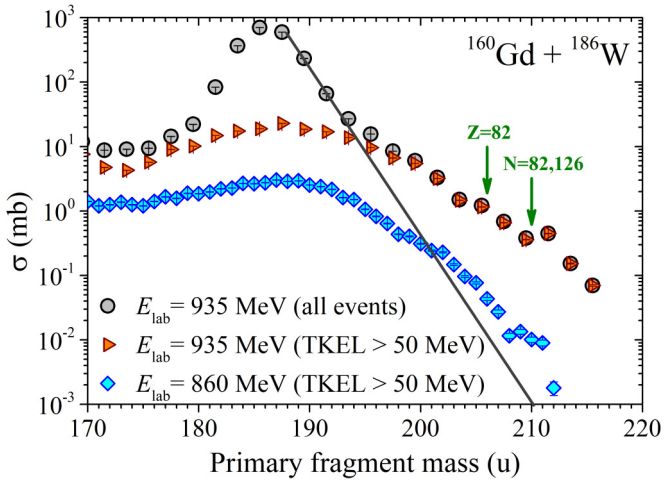

FIG. 10. Mass distribution for all binary events (circles) formed in the reaction ^{160}Gd + ^{186}W at E_{lab} = 935 MeV, and mass distributions of fragments with TKEL > 50 MeV formed in the ^{160}Gd + ^{186}W reaction at E_{lab} = 935 MeV (triangles) and E_{lab} = 860 MeV (diamonds). The arrows indicate the positions of neutron and proton shells.

V. SUMMARY

The mass, energy, and angular distributions of fragments formed in the reactions ^{156,160}Gd + ^{186}W at E_{lab} = 878 MeV in the case of ^{156}Gd ions and E_{lab} = 860, 935 MeV for ^{160}Gd ions have been measured to study the influence of the closed proton and neutron shells on the formation of reaction products in the inverse QF process. The enhanced yield of products with masses 200–215 u (mass transfer of 20–25 nucleons) was observed for both reactions ^{156,160}Gd + ^{186}W at energies near the Coulomb barrier for interaction of spherical nuclei. The cross sections of the formation of trans-target fragments heavier than 200 u in the reactions ^{156,160}Gd + ^{186}W at this energy are found to be about 10 μb. Although the formation cross sections of these fragments are approximately the same for both reactions, in the case of the ^{160}Gd-induced reaction the excitation energy is 10–20 MeV lower than in the case of ^{156}Gd. It leads to a lower number of neutrons emitted during the deexcitation process in the former reaction. Thus, the reaction with ^{160}Gd ions is more suitable for producing neutron-rich nuclei in the inverse QF process.

The orientation effect caused by the strong deformation of colliding nuclei plays an important role in the formation of the reaction fragments that can result in a gain in the yield of trans-target fragments. The analysis of mass, energy, and angular distributions of fragments formed in the reaction ^{160}Gd + ^{186}W at an energy of 935 MeV, which is above the barrier for side-to-side collisions and for which all the orientations of interacting nuclei are possible, has shown that the formation cross section of fragments with mass ∼208 u is about 50 times higher than in the case of measurements near the Coulomb barrier energy, while the excitation energies of these fragments, on average, increase insignificantly.

This enhancement, found in the yield of products with masses heavier than the target mass, confirms the important role of closed shells in the inverse quasifission process in low-energy damped collisions. Thereby, low-energy multinucleon transfer reactions are a promising pathway for producing new neutron-rich isotopes.

For further progress in obtaining new neutron-enriched isotopes of heavy and superheavy nuclei in the quasifission and multinucleon transfer reactions, additional investigations are needed to optimize the choice of the reaction partners, the energy of bombarding particles, and the registration angles.

ACKNOWLEDGMENTS

We thank the staff of the U400 cyclotron for their careful work. We acknowledge with deep gratitude the constant interest in the experiments and support of the directorate of the FLNR JINR. This work was supported by the Russian Foundation for Basic Research (Grant No. 13-02-01282-a).

[1] E. M. Kozulin, G. N. Knyazheva, K. V. Novikov, I. M. Itkis, M. G. Itkis, S. N. Dmitriev, Y. T. Oganessian, A. A. Bogachev, N. I. Kozulina, I. Harca, W. H. Trzaska, and T. K. Ghosh, Phys. Rev. C **94**, 054613 (2016).
[2] M. G. Itkis, E. Vardaci, I. M. Itkis, G. N. Knyazheva, and E. M. Kozulin, Nucl. Phys. A **944**, 204 (2015).
[3] V. I. Zagrebaev, Yu. Ts. Oganessian, M. G. Itkis, and W. Greiner, Phys. Rev. C **73**, 031602(R) (2006).
[4] V. Zagrebaev and W. Greiner, J. Phys. G **34**, 2265 (2007).
[5] V. Zagrebaev and W. Greiner, Phys. Rev. Lett. **101**, 122701 (2008).
[6] V. I. Zagrebaev and W. Greiner, Phys. Rev. C **83**, 044618 (2011).
[7] A. V. Karpov and V. V. Saiko, Phys. Rev. C **96**, 024618 (2017).
[8] http://nrv.jinr.ru/nrv
[9] W. Loveland, A. M. Vinodkumar, D. Peterson, and J. P. Greene, Phys. Rev. C **83**, 044610 (2011).
[10] E. M. Kozulin, G. N. Knyazheva, S. N. Dmitriev, I. M. Itkis, M. G. Itkis, T. A. Loktev, K. V. Novikov, A. N. Baranov, W. H. Trzaska, E. Vardaci, S. Heinz, O. Beliuskina, and S. V. Khlebnikov, Phys. Rev. C **89**, 014614 (2014).
[11] E. M. Kozulin *et al.*, Instrum. Exp. Tech. **51**, 44 (2008).
[12] I. M. Itkis, E. M. Kozulin, M. G. Itkis, G. N. Knyazheva, A. A. Bogachev, E. V. Chernysheva, L. Krupa, Y. T. Oganessian, V. I. Zagrebaev, A. Y. Rusanov, F. Goennenwein, O. Dorvaux, L. Stuttge, F. Hanappe, E. Vardaci, and E. deGoesBrennand, Phys. Rev. C **83**, 064613 (2011).
[13] W. W. Wilcke, J. R. Birkelund, A. D. Hoover, J. R. Huizenga, W. U. Schröder, V. E. Viola, K. L. Wolf, and A. C. Mignerey, Phys. Rev. C **22**, 128 (1980).
[14] C. Riedel, G. Wolschin, and W. Nörenberg, Z. Phys. A **290**, 47 (1979).
[15] J. Stroth *et al.*, Z. Phys. A **357**, 441 (1997).
[16] C. Golabek *et al.*, Eur. Phys. J. A **43**, 251 (2010).
[17] V. V. Volkov, Phys. Rep. **44**, 93 (1978).
[18] E. M. Kozulin, E. Vardaci, G. N. Knyazheva, A. A. Bogachev, S. N. Dmitriev, I. M. Itkis, M. G. Itkis, A. G. Knyazev, T. A. Loktev,

K. V. Novikov, E. A. Razinkov, O. V. Rudakov, S. V. Smirnov, W. Trzaska, and V. I. Zagrebaev, Phys. Rev. C **86**, 044611 (2012).

[19] J. Wilczynski and H. W. Wilschut, Phys. Rev. C **39**, 2475 (1989).

[20] D. J. Hinde, M. Dasgupta, J. R. Leigh, J. C. Mein, C. R. Morton, J. O. Newton, and H. Timmers, Phys. Rev. C **53**1290 (1996).

[21] G. N. Knyazheva, E. M. Kozulin, R. N. Sagaidak, A. Y. Chizhov, M. G. Itkis, N. A. Kondratiev, V. M. Voskressensky, A. M. Stefanini, B. R. Behera, L. Corradi, E. Fioretto, A. Gadea, A. Latina, S. Szilner, M. Trotta, S. Beghini, G. Montagnoli, F. Scarlassara, F. Haas, N. Rowley, P. R. S. Gomes, and A. SzantodeToledo, Phys. Rev. C **75**, 064602 (2007).

[22] V. Zagrebaev and W. Greiner, Int. J. Mod. Phys. E **17**, 2199 (2008).

[23] K. Nishio, H. Ikezoe, S. Mitsuoka, I. Nishinaka, Y. Nagame, Y. Watanabe, T. Ohtsuki, K. Hirose, and S. Hofmann, Phys. Rev. C **77**, 064607 (2008).

[24] A. Wakhle, C. Simenel, D. J. Hinde, M. Dasgupta, M. Evers, D. H. Luong, R. du Rietz, and E. Williams, Phys. Rev. Lett. **113**, 182502 (2014).

[25] V. Zagrebaev, A. Karpov, Y. Aritomo, M. Naumenko, and W. Greiner, Phys. Part. Nucl. **38**, 469 (2007).

[26] A. B. Migdal, *The Theory of Finite Fermi-Systems and Properties of Atomic Nuclei*, 2nd ed. (Nauka, Moscow, 1983), in Russian; J. Speth, E. Werner, and W. Wild, Phys. Rep. **33**, 127 (1977).